Handout # 14 (MEEN 626) **Application example**

Experimental identification of bearing force coefficients

Experimental identification of the dynamic force coefficients of bearings, seals and other rotor support elements is of importance (a) to predict, at the design stage, the dynamic force performance of a rotor using these elements; (b) to reproduce rotordynamic performance when troubleshooting rotor-bearing system malfunctions or searching for instability sources; and (c) to validate (and calibrate) predictive tools for bearing and seal analyses. The ultimate goal is to collect e a reliable data base from which to determine the confidence of bearing and/or seal operation under both normal design conditions and extreme environments due to unforeseen events.

In addition, even advanced predictive computational physics based models are very limited or non-existing for certain bearing and seal configurations and with stringent particular operating conditions, and thus experimental measurement of the actual element force coefficients constitute the only option available to generate engineering results of interest. Squeeze film dampers operating with persistent air ingestion and entrapment are an application example where systematic experimentation becomes mandatory.

The widespread availability and low-cost of PC high-speed data acquisition equipment and (real time) data signal processing have promoted dramatic advancements in the field of bearing and seal parameter identification. In most cases, methods are restricted to the laboratory environment and strictly applicable to rigid rotor configurations and identical bearing supports. Time and frequency

domain based parameter identification procedures are based on the seminal works of Goodwin [1991] and Nordmann [1980], respectively.

Tiwari, R., Lees, A.W., Friswell, M.I. 2004. "Identification of Dynamic Bearing Parameters: A Review." *The Shock and Vibration Digest*, **36,** pp. 99-124.

The paper reviews the most popular test techniques and analysis methods to identify linearized force coefficients in fluid film bearings. The methods include time and frequency domain procedures, while experimentation focuses on the types of dynamic load excitation most efficient for a particular procedure. The review also includes physics based mathematical modeling with governing equations of the test bearing element or rotor-bearing system, parameter extraction algorithms, and uncertainty in the estimates. The classification of identification techniques is based on the method used to excite the test element or system: short duration (impacts and shock loads), periodic load excitation, fixed or sine-sweep and including imbalance induced forces, and random load excitation techniques.

Identification algorithms consider the test bearing or support as a two degree of freedom mechanical system undergoing lateral motions $(x,\ y)_{(t)}$ and with readily available (measured) support transmitted forces and rotor displacements from which test impedances or mobilities are obtained. Curve fits to the appropriate transfer functions give the support mechanical parameters.

For lateral rotor motions (x, y), a bearing or seal reaction force vector $\mathbf{f}$ is usually modeled as

$$\begin{bmatrix} f_{X_{(t)}} \\ f_{Y_{(t)}} \end{bmatrix} = \begin{bmatrix} f_{Xo} \\ f_{Yo} \end{bmatrix} - \begin{bmatrix} K_{XX} & K_{XY} \\ K_{YX} & K_{YY} \end{bmatrix} \begin{bmatrix} X_{(t)} \\ Y_{(t)} \end{bmatrix} - \begin{bmatrix} K_{XX} & K_{XY} \\ K_{YX} & K_{YY} \end{bmatrix} \begin{bmatrix} x_{(t)} \\ y_{(t)} \end{bmatrix} - \begin{bmatrix} C_{XX} & C_{XY} \\ C_{YX} & C_{YY} \end{bmatrix} \begin{bmatrix} \dot{x}_{(t)} \\ \dot{y}_{(t)} \end{bmatrix} - \begin{bmatrix} M_{XX} & M_{XY} \\ M_{YX} & M_{YY} \end{bmatrix} \begin{bmatrix} \ddot{x}_{(t)} \\ \ddot{y}_{(t)} \end{bmatrix} \tag{1.1}$$

or

$$\mathbf{f}_{(t)} = \begin{bmatrix} \mathbf{f_X} \\ \mathbf{f_Y} \end{bmatrix} = \mathbf{f_o} - \mathbf{K}\,\mathbf{x} - \mathbf{C}\,\dot{\mathbf{x}} - \mathbf{M}\,\ddot{\mathbf{x}} \quad \text{with} \quad \mathbf{x}_{(t)} = \begin{bmatrix} x \\ y \end{bmatrix} \tag{1.2}$$

where $\mathbf{f_o}$ is a static equilibrium force typically counteracting a fraction of the rotor weight, for example. The test element force coefficients are four (4) stiffness K and four (4) damping C force coefficients in mineral oil lubricated bearings, oil seals, and also gas damper seals. In liquid annular (damper) seals and bearings (hydrostatic and/or hydrodynamic) working with process fluids (water or LOx, for example), four (4) inertia force coefficients M are also important.

Please note that these force coefficients (K, C, M) are mechanical parameters representative of a **linear or** rather **linearinzed physical system.** In this regard, the (K, C, M) coefficients are to be determined in a system or test element undergoing small amplitude motions about an equilibrium condition. This operating condition is of utmost importance to obtain reliable and repeatable results. Unfortunately, the basic assumption – needed to ensure the physical model is linear- is

often not considered by the experimenters, and which explains the vast differences in parameter magnitudes when compared to analytical model predictions, for example.

Incidentally, the linearized coefficient model for the test element, i.e. a bearing or a seal or a support, also assumes that the **coefficients are frequency independent**. Only in the last 10 years, since the late 1990's, the engineering community has recognized this limitations and developed techniques to extract parameters from frequency domain measurements.

Furthermore, note that the so called "experimental" force coefficients (*K, C, M*) are in actuality not measured parameters but mere ESTIMATIONS derived from procedures (ranging from simple or complex) that relate motions of the test system or element due to known applied forces.

Until recently, estimation of bearing and seal rotordynamic force coefficients was traditionally based on time domain response methods. These techniques, often limited in scope, use only a limited amount of the recorded information rendering poor results with marginal confidence levels. **Modern parameter identification techniques** are based on **frequency domain procedures**, where dynamic force coefficients are estimated from **transfer functions of measured** displacements (velocities and accelerations as well) due to **external loads of a prescribed time varying structure.** Frequency domain methods take advantage of high speed computing and digital signal processors, thus producing estimates of system parameters in real time and at a fraction of the cost (and effort) with cumbersome time domain algorithms.

Consider a test bearing or seal element as a point mass undergoing forced vibrations induced by external forcing functions.

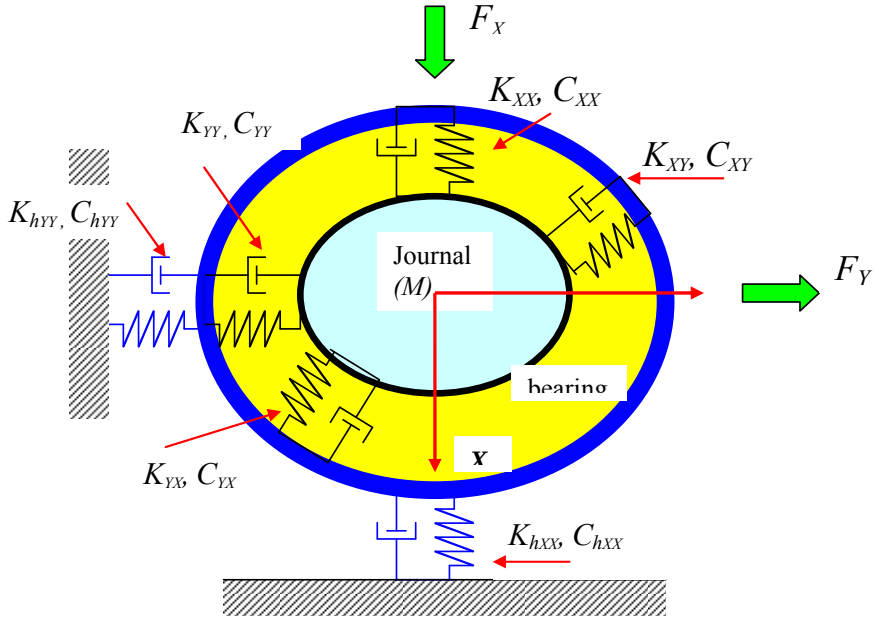

Representation of point mass and bearing force coefficients used for identification of parameters from dynamic load and motion measurements

For small amplitudes about an equilibrium position, the equations of motion of a linear mechanical system are

$$M_h\ddot{x} + \left(C_{XX} + C_{hX}\right)\dot{x} + C_{XY}\dot{y} + \left(K_{XX} + K_{hX}\right)x + K_{XY}y = f_X$$

$$M_h\ddot{y} + \left(C_{YY} + C_{hY}\right)\dot{y} + C_{YX}\dot{x} + \left(K_{YY} + K_{hY}\right)y + K_{YX}x = f_Y \qquad (2)$$

where

$\{f_i\}_{i=X,Y}$	external excitation forces,
M_h	test element mass,
$\{K_{hi},\ C_{hi}\}_{i=X,Y}$	(any) structural support stiffness and remnant damping coefficients[1], and
$\{K_{ij},\ C_{ij}\}_{i,j=X,Y}$	seal or bearing dynamic stiffness and damping force coefficients.

Inertia force coefficients are not included in the model above. Added mass coefficients are NOT significant, i.e. their magnitude is small, for highly compressible fluids (LH_2 or gases) and in most bearing and seals lubricated with mineral oil[2]. The apparent simplification is easily removed and does not diminish the importance of the identification method. The test system structural stiffness and damping coefficients, $\{K_{hi}, C_{hi}\}_{i=X,Y}$, are obtained from prior shake tests results under dry conditions, i.e. without fluid through the test element

Two independent force excitations (impact, periodic-single frequency, sine-swept, random, etc) $(f_X, 0)^T$ and $(0, f_Y)^T$, for example, are applied to the test element. This process is formulated as

1. Apply $\begin{bmatrix} f_{x_1} \\ f_{y_1} \end{bmatrix}_{(t)}$ and measure $\begin{bmatrix} x_{1_{(t)}} \\ y_{1_{(t)}} \end{bmatrix}$ (3a); apply $\begin{bmatrix} f_{x_2} \\ f_{y_2} \end{bmatrix}_{(t)}$ and measure $\begin{bmatrix} x_{2_{(t)}} \\ y_{2_{(t)}} \end{bmatrix}$ (3b)

[1] Refers to any mechanical component assisting to support the test bearing, for example connecting rods or springs; and damping from the test system DRY, i.e. without any lubricant, for example.

[2] Note that test data by Childs et al. obtained for mineral oil tilting pad bearings, pressure dam bearings and floating ring seals actually evidence these test elements show large added mass coefficients; larger in magnitude than theoretical model predictions. See Notes 7 or Notes 11 for further details and discussion.

2. Obtain the **discrete Fourier transform (DFT)**[3] of the applied forces and displacements, i.e. Let

$$\begin{bmatrix} F_{X_{1(\omega)}} \\ F_{Y_{1(\omega)}} \end{bmatrix} = DFT \begin{bmatrix} f_{x_{1(t)}} \\ f_{Y_{1(t)}} \end{bmatrix}; \begin{bmatrix} X_{1(\omega)} \\ Y_{1(\omega)} \end{bmatrix} = DFT \begin{bmatrix} x_{1(t)} \\ y_{1(t)} \end{bmatrix}; \tag{4a}$$

$$\begin{bmatrix} F_{X_{2(\omega)}} \\ F_{Y_{2(\omega)}} \end{bmatrix} = DFT \begin{bmatrix} f_{x_{2(t)}} \\ f_{Y_{2(t)}} \end{bmatrix}; \begin{bmatrix} X_{2(\omega)} \\ Y_{2(\omega)} \end{bmatrix} = DFT \begin{bmatrix} x_{2(t)} \\ y_{2(t)} \end{bmatrix} \tag{4b}$$

The DFT is an operation that transforms the information from the **time domain** into the **frequency domain**. Incidentally, recall that

$$i\,\omega\, X_{(\omega)} = DFT\left[\dot{x}_{(t)}\right]; \quad -\omega^2\, X_{(\omega)} = DFT\left[\ddot{x}_{(t)}\right] \tag{5}$$

---

[3] A sequence of *N* time-domain data points, say $[(z_1,t_1=0), (z_2,t_2), \ldots. (z_N,t_N=t_{max})]$ and with $\Delta t=t_2-t_1= t_3-t_2=\ldots$, will transform, using the DFT algorithm, into ½ *N* coefficients (complex numbers with amplitude and phase) at discrete frequencies $Z_k=a_k e^{i\phi_k}$ at discrete frequencies $\omega_0=0$, $\omega_1=\delta_\omega$, $\omega_2=2\delta_\omega$,….. $\omega_{N/2}=½\ N\ \delta_\omega= \omega_{max}= 1/(2\Delta t)$. Hence, $\delta_\omega=1/(N\ \Delta t) \sim 1/t_{max}$. Typically, *N* is a power of 2, i.e. *N*=256, 512, etc for efficient and fast data processing. Note that $1/\Delta t$ is known as the **sampling rate.** In addition, **the longer the time span for analysis (t_{max}), the smaller is the frequency step (δ_ω); while the faster the data acquisition sampling rate,** Δt is small, the highest is the maximum frequency (ω_{max}) of the DFT. Satisfying both small δ_ω and very high ω_{max} may require of exceedingly large number of data points. Often, these two conditions can not be attained simultaneously; and in which case care is needed to avoid aliasing of the recorded signal as well as other spurious effects. Read a dedicated book in Fast Fourier Transform analysis for more accurate and relevant details.

3. For the **assumed** physical model, the motion ODEs become for the first test set and in the frequency domain:

$$-M_h\omega^2 X_1 + \left(C_{XX} + C_{hX}\right) i\omega X_1 + C_{XY} i\omega Y_1 + \left(K_{XX} + K_{hX}\right) X_1 + K_{XY} Y_1 = F_{X_1}$$

$$-M_h\omega^2 Y_1 + \left(C_{YY} + C_{hY}\right) i\omega Y_1 + C_{YX} i\omega X_1 + \left(K_{YY} + K_{hY}\right) Y_1 + K_{YX} X_1 = F_{Y_1} \quad (6)$$

Or, written in matrix form as

$$\begin{bmatrix} K_{XX} + K_{hX} - M_h\omega^2 + i\omega\left(C_{XX} + C_{hX}\right) & K_{XY} + i\omega C_{XY} \\ K_{YX} + i\omega C_{YX} & K_{YY} + K_{hY} - M_h\omega^2 + i\omega\left(C_{YY} + C_{hY}\right) \end{bmatrix} \begin{Bmatrix} X_1 \\ Y_1 \end{Bmatrix} = \begin{Bmatrix} F_{X_1} \\ F_{Y_1} \end{Bmatrix}$$

Define **complex impedances**[4] $\{H_{ij}\}_{i,j=X,Y}$ as

$$H_{ij} = \left[\left(K_{ij} + K_{hi}\delta_{ij}\right) - \omega^2 M_{hi}\delta_{ij}\right] + i\omega\left(C_{ij} + C_{hi}\delta_{ij}\right) \quad (7)$$

where $i = \sqrt{-1}$, $\delta_{ij} = 1$ for $i = j = X, Y$; zero otherwise.

[4] As you know well, impedance is a misnomer. Dynamic (complex) stiffness is a more appropriate name.

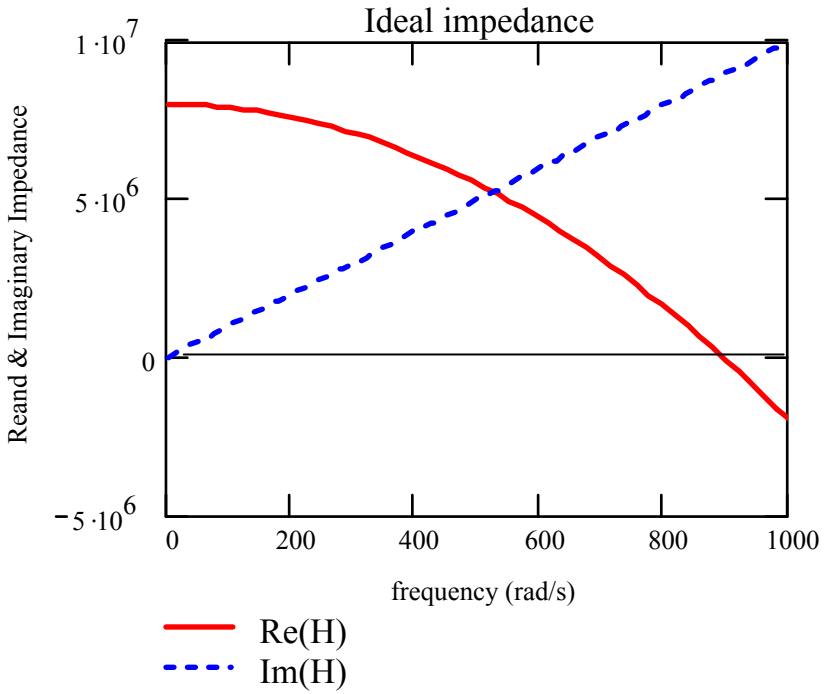

The impedances comprise real and imaginary parts, both functions of the excitation frequency (ω). The real part denotes the dynamic stiffness, while the imaginary part (quadrature stiffness) is proportional to the *viscous* damping coefficient, as shown in the figure.

xx

Real and imaginary parts of ideal mechanical impedance representative of assumed physical model

With definition (7), the EOMs (6) become, for the first & second tests,

$$\begin{bmatrix} H_{XX_{(\omega)}} & H_{XY_{(\omega)}} \\ H_{YX_{(\omega)}} & H_{YY_{(\omega)}} \end{bmatrix} \begin{Bmatrix} X_1 \\ Y_1 \end{Bmatrix} = \begin{Bmatrix} F_{X_1} \\ F_{Y_1} \end{Bmatrix} \quad \text{and} \quad \begin{bmatrix} H_{XX_{(\omega)}} & H_{XY_{(\omega)}} \\ H_{YX_{(\omega)}} & H_{YY_{(\omega)}} \end{bmatrix} \begin{Bmatrix} X_2 \\ Y_2 \end{Bmatrix} = \begin{Bmatrix} F_{X_2} \\ F_{Y_2} \end{Bmatrix} \tag{6a}$$

Add these two equations and reorganize them as

$$\begin{bmatrix} H_{XX} & H_{YX} \\ H_{XY} & H_{YY} \end{bmatrix} \begin{bmatrix} X_1 & X_2 \\ Y_1 & Y_2 \end{bmatrix} = \begin{bmatrix} F_{X_1} & F_{X_2} \\ F_{Y_1} & F_{Y_2} \end{bmatrix} \tag{8}$$

At each frequency ($\omega_{k=1,2,\ldots n}$), Eq. (8) represents **four independent equations** with **four unknowns**, $(H_{XX}, H_{YY}, H_{XY}, H_{YX})$. Hence,

$$\begin{bmatrix} H_{XX} & H_{YX} \\ H_{XY} & H_{YY} \end{bmatrix} = \begin{bmatrix} F_{X_1} & F_{X_2} \\ F_{Y_1} & F_{Y_2} \end{bmatrix} \begin{bmatrix} X_1 & X_2 \\ Y_1 & Y_2 \end{bmatrix}^{-1} \tag{9a}$$

$$\mathbf{H} = \begin{bmatrix} \mathbf{F}^{(1)} & \mathbf{F}^{(2)} \end{bmatrix} \begin{bmatrix} \mathbf{X}^{(1)} & \mathbf{X}^{(2)} \end{bmatrix}^{-1} \quad \text{where} \quad \mathbf{F}^{(1)} = \begin{bmatrix} F_{X_1} \\ F_{Y_1} \end{bmatrix} \& \ \mathbf{X}^{(1)} = \begin{bmatrix} X_1 \\ Y_1 \end{bmatrix}, \ \mathbf{F}^{(2)} = \begin{bmatrix} F_{X_2} \\ F_{Y_2} \end{bmatrix} \& \ \mathbf{X}^{(2)} = \begin{bmatrix} X_2 \\ Y_2 \end{bmatrix} \tag{9b}$$

The **meaning of linear independence** of the test forces (and ensuing motions) should now be clear. That is, the forces in the second test cannot be a multiple of the first set of forces since then, both the matrix of forces $[\mathbf{F}^{(1)}\ \mathbf{F}^{(2)}]$ and the matrix of ensuing displacements $[\mathbf{X}^{(1)}\ \mathbf{X}^{(2)}]$ become **singular**.

The experimenter must select sets of excitations that are linearly independent, for example $(f_X, 0)^T$ and $(0, f_Y)^T$ are preferred (and easy) choices.

In the identification process, the importance of linear independence in the application of forces and ensuing test system or bearing displacements is MOST important to obtain reliable and

repeatable results. In actual practice, measured displacements may not appear similar to each other but nonetheless produce an identification matrix that is ill conditioned, i.e., the determinant of matrix $\mathbf{[X^{(1)}\ X^{(2)}]}$ is close to zero or is zero. In this case, the **condition number of the identification matrix** is of importance to determine whether the identified coefficients are any good. Test elements that are nearly isotropic and that are excited by periodic (single frequency) loads producing circular orbits of the test system usually determine a too *ill conditioned* system (Murphy, 1990).

Often enough the calculation of the matrix $\mathbf{[X^{(1)}\ X^{(2)}]}$ condition number and checking for ill-conditioning is easily overlooked.

Preliminary estimates of the system parameters $\{M,\ K,\ C\}_{i,j=X,Y}$ are determined by curve fitting of the test derived discrete set of impedances $(H_{XX},\ H_{YY},\ H_{XY},\ H_{YX})_{k=1,2....}$, one set for each frequency ω_k, to the analytical formulas over a pre-selected frequency range. That is, for example

$$\left(K_{XX}+K_{hX}\right)-\omega^2 M_h=\text{Real}\left(H_{XX}\right) \qquad \omega\left(C_{XX}+C_{hX}\right)=\text{Ima}\left(H_{XX}\right) \qquad (10)$$

Since 1993, Childs and students excel in employing the impedance identification method to "measure" rotordynamic force coefficients in hydrostatic bearings and annular seals with water as the lubricant (Rouvas and Childs, 1993). The method lends itself to simple curve-fitting of the recorded impedance functions H to physically representative analytical functions, i.e. $K\text{-}\omega^2 M$ and ωC.

Analytical curve fitting of any data renders a **correlation coefficient** (r^2) representing the goodness of the fit. A low value of the correlation coefficient, $r^2 << 1$, does not mean the test data or the obtained impedance are incorrect, but rather that the physical model (analytical function) chosen to represent the test system does not actually reproduce the measurements. On the other hand, a high $r^2 \sim 1$ demonstrates that the physical model, say with a constant stiffness K and viscous damping C in $K-\omega^2 M$ and ωC, respectively, actually describes the measurements (system response) with accuracy.

System transfer functions (output/input) are often used to obtain **more precise estimates** of the seal or bearing force coefficients (Nordmann and Schollhorn, 1980, Massmann and Nordmann, 1985). This process leads to curve fits of nonlinear functions.

Transfer functions (displacement/force) known as **test system flexibilities G** are derived as functions of the impedances, $(H_{ij})_{i,,j=X,Y}$ from the fundamental equation $\mathbf{G = H^{-1}}$, i.e.

$$G_{XX} = TF(X_1) = \frac{H_{YY}}{\Delta}; \quad G_{XY} = TF(X_2) = \frac{-H_{XY}}{\Delta}$$

$$G_{YX} = TF(Y_1) = \frac{-H_{YX}}{\Delta}; \quad G_{YY} = TF(Y_2) = \frac{H_{XX}}{\Delta} \qquad (11a)$$

where

$$\Delta = H_{XX} H_{YY} - H_{XY} H_{YX} \qquad (11c)$$

Next, the **Instrumental Variable Filter (IVF) method** of Fritzen (1985), an extension of a **least-squares estimation** method, is used to simultaneously curve fit all four transfer functions from motion measurements due to two sets of (linearly independent) applied loads. **The IVF method has the advantage of eliminating bias typically seen in an estimator due to measurement noise.**

The product of the flexibility (**G**) and impedance (**H**) matrices should be identically equal to the identity matrix $\mathbf{I}=\begin{bmatrix}1 & 0\\ 0 & 1\end{bmatrix}$ since $\mathbf{G}=\mathbf{H}^{-1}$.

However, in any measurement process there is some noise associated with the experiments. Thus, an **error matrix** (**e**) is introduced into the fundamental relationship,

$$\mathbf{G}\cdot\mathbf{H}=\mathbf{G}\left[\mathbf{K}-\omega^2\mathbf{M}+i\,\omega\mathbf{C}\right]=\mathbf{I}+\mathbf{e} \qquad (12)$$

where **K, C** and **M** are matrices of system stiffness, damping and added mass coefficients.

$$\mathbf{K}=\begin{bmatrix}K_{XX}+K_{hX} & K_{XY}\\ K_{YX} & K_{YY}+K_{hY}\end{bmatrix},\mathbf{C}=\begin{bmatrix}C_{XX}+C_{hX} & C_{XY}\\ C_{YX} & C_{YY}+C_{hY}\end{bmatrix},\ \mathbf{M}=\begin{bmatrix}M_{XX}+M_{h} & M_{XY}\\ M_{YX} & M_{YY}+M_{h}\end{bmatrix}$$

For generality, added mass coefficients (M_{XX}, M_{YY}, M_{XY}, M_{YX}) are included in the matrices above.

In Eq. (12) **G** denotes the **measured flexibility matrix** while **H** represents the (to be) estimated test system impedance as defined in Eq. (7). **Recall that Eq. (7) corresponds to the physical model ASSUMED to best represent the test system or test element.**

In the present method, the flexibility coefficients (**G**) work as weight functions of the errors in a minimization procedure. Whenever the flexibility coefficients are large, the error is also penalized by a larger value. As a result, the minimization procedure will become better in the neighborhood of the system resonances (natural frequencies) where the dynamic flexibilities are maxima (i.e., null dynamic stiffness, $(K-\omega^2 M)=0$. That is, the measurements containing resonance regions will have more weight on the fitted system parameters. External forcing functions exciting the test system resonances are more reliable because at those frequencies the system is more sensitive, and the measurements are accomplished with larger signal to noise ratios.

In addition, it is precisely around the resonant frequencies where all the physical parameters (mass, damping and stiffness) most affect appreciably the system response. For "too low" frequencies the important parameter is the stiffness, while for "too high" frequencies the inertia dominates the response. Only near the resonance do all three parameters have an important effect on the system amplitude response.

Therefore, it is **more accurate to minimize the approximation errors** using Eq. (12) rather than directly curve fitting the impedances, i.e. simply using Eq. (10). Unfortunately, the process is not straightforward and leads to a rather complex minimization scheme.

Write the impedance matrix $\mathbf{H}$ representing the test system or test element as

$$\mathbf{H}_{(\omega)} = \left[-\omega^2 \mathbf{I} \,\vdots\, i\,\omega \mathbf{I} \,\vdots\, \mathbf{I} \right] \begin{bmatrix} \mathbf{M} \\ \mathbf{C} \\ \mathbf{K} \end{bmatrix} \tag{14}$$

with $i = \sqrt{-1}$ and $\mathbf{I} = \begin{bmatrix} 1 & 0 \\ 0 & 1 \end{bmatrix}$. Thus Eq. (12) becomes at each discrete frequency $\omega_{k=1,2\ldots,n}$

$$\mathbf{G}^k \left[-\omega_k^2 \mathbf{I} \,\vdots\, i\,\omega_k \mathbf{I} \,\vdots\, \mathbf{I} \right] \begin{bmatrix} \mathbf{M} \\ \mathbf{C} \\ \mathbf{K} \end{bmatrix} = \mathbf{I} + \mathbf{e}^k \tag{15a}$$

Let

$$\mathbf{A}^k = \mathbf{G}^k \left[-\omega_k^2 \mathbf{I} \,\vdots\, i\,\omega_k \mathbf{I} \,\vdots\, \mathbf{I} \right] \tag{16}$$

And write Eq. (15a) as

$$\mathbf{A}^k \begin{bmatrix} \mathbf{M} \\ \mathbf{C} \\ \mathbf{K} \end{bmatrix} = \mathbf{I} + \mathbf{e}^k \tag{15b}$$

Now, stack all the equations, one for each frequency $\omega_{k=1,2\ldots,n}$, to obtain the set

$$\underline{\mathbf{A}} \begin{bmatrix} \mathbf{M} \\ \mathbf{C} \\ \mathbf{K} \end{bmatrix} = \underline{\mathbf{I}} + \underline{\mathbf{e}} \tag{17}$$

where $\underline{\mathbf{A}} = \begin{bmatrix} \mathbf{A}^1 \\ \mathbf{A}^2 \\ \mathbf{A}^n \end{bmatrix}$, $\underline{\mathbf{e}} = \begin{bmatrix} \mathbf{e}^1 \\ \mathbf{e}^2 \\ \mathbf{e}^n \end{bmatrix}$ and $\underline{\mathbf{I}}^T = \begin{bmatrix} 0 & 1 & 0 & 1 & 0 & 1 & .. & .. & .. & .. & 0 & 1 \\ 1 & 0 & 1 & 0 & 1 & 0 & .. & .. & .. & .. & 1 & 0 \end{bmatrix}$ (18)

$\underline{\mathbf{A}}$ contains the stack of measured flexibility functions (at discrete frequencies $\omega_{k=1,2\ldots,n}$). Eq. (17) is an over determined set of equations, i.e. there are more equations than unknowns. Hence, its **solution by least-squares aims to minimize the Euclidean norm of $\underline{\mathbf{e}}$. This minimization leads to the normal equations,**

$$\begin{bmatrix} \mathbf{M} \\ \mathbf{C} \\ \mathbf{K} \end{bmatrix} = \left(\underline{\mathbf{A}}^{\mathbf{T}} \underline{\mathbf{A}} \right)^{-1} \underline{\mathbf{A}}^{\mathbf{T}} \underline{\mathbf{I}} \tag{19}$$

A first set of force coefficients (**M,C,K**) is determined from these equations.

Fritzen (1985) introduced the elegant **Instrumental Variable Filter Method (*IVF*)** to solve the system coefficients that minimize the Euclidean (L^2) norm of the system error $\underline{\mathbf{e}}$. The IVF procedure was originally developed to estimate parameters in econometric problems. Massmann and Nordmann (1985) applied successfully the method to fluid film annular seal elements.

In the **IVF** method, the weighting function, $\underline{\mathbf{A}}$, is replaced by a new matrix function, $\underline{\mathbf{W}}$, created from the analytical flexibilities resulting from the (initial) least-squares curve fit, i.e., solution of Eq. (19). **This weighting function $\underline{\mathbf{W}}$ is free of measurement noise** and contains peaks only at the resonant frequencies as determined from the first estimates of stiffness, mass and damping force coefficients.

At step *m,*

$$\begin{bmatrix} \mathbf{M} \\ \mathbf{C} \\ \mathbf{K} \end{bmatrix}^{m+1} = \left(\left[\underline{\mathbf{W}}^m \right]^T \underline{\mathbf{A}} \right)^{-1} \left[\underline{\mathbf{W}}^m \right]^T \underline{\mathbf{I}} \tag{20}$$

where

$$\underline{\mathbf{W}}^m = \begin{bmatrix} \left[\underline{\bar{\mathbf{F}}}^m_{(\omega_1)} \left[-\omega_1^2 \mathbf{I} \mid i\omega_1 \mathbf{I} \mid \mathbf{I} \right] \right] \\ \vdots \\ \left[\underline{\bar{\mathbf{F}}}^m_{(\omega_n)} \left[-\omega_n^2 \mathbf{I} \mid i\omega_n \mathbf{I} \mid \mathbf{I} \right] \right] \end{bmatrix}$$

and

$$\underline{\bar{\mathbf{F}}}^m_{(\omega)} = \left[\left[-\omega^2 \mathbf{I} \mid i\,\omega \mathbf{I} \mid \mathbf{I} \right] \begin{bmatrix} \mathbf{M} \\ \mathbf{C} \\ \mathbf{K} \end{bmatrix}^m \right]^{-1} \tag{21}$$

A first iteration (m=1) is performed with $\mathbf{W}^1=\mathbf{A}$, which corresponds to the standard least-squares solution of the problem, eq. (19). Then, Eqs. (20) and (21) are applied iteratively until a given convergence criterion or tolerance is satisfied. This criterion can be conveniently chosen depending on the desired results. For example, the square summation of the differences between the parameters at iteration m and (m-1) can be required to be less than a certain value, i.e. limiting the Euclidean norm of the error. Alternatively, it can be required that the largest difference be less than the largest acceptable error, i.e. limiting the L_1 norm of the error. Different tolerances to each variable could also be asserted depending on their physical units and significance.

It should be clear that the substitution of $\mathbf{W}$ for the discrete measured flexibility $\mathbf{A}$ (which also contains noise) improves the prediction of the system parameters. Note that the product $\mathbf{A}^T\mathbf{A}$ amplifies the noisy components and adds them. Therefore, even if the noise has a zero mean value, the addition of its squares becomes positive resulting in a bias error. On the other hand, $\mathbf{W}$ does not have components correlated to the measurement noise. That is, no **bias error** is kept in the product $\mathbf{W}^T\mathbf{A}$. Consequently, the approximation to the system parameters is improved.

Note that the force coefficients are identified in the frequency domain. Thus, magnitudes of uncertainty for the estimated force coefficients must be obtained by comparing the original frequency responses with the frequency response of a reference excitation force and associated displacement time response. Evaluation of coherence functions then becomes necessary to reproduce the exact variability of the identified force coefficients.

Closure

Read the paper of Diaz and San Andrés (1999) – following pages- for further insight on the IVF method as applied to a *n-DOF* system. A MATHCAD® program is available for your self-study and further learning.

An example of parameter identification representative of your lecturer's research will be presented in class.

Recent developments on field or in-situ parameter identification methods

Field identification of fluid film bearing parameters is critical for adequate interpretation of rotating machinery performance and necessary to validate or calibrate predictions from restrictive computational fluid film bearing models. The key features of a successful method for ready field implementation are minimal external equipment, little or no changes to existing hardware, and the use of measuring instruments commonly used in machine protection and monitoring.

DeSantiago and San Andrés (2004, 2007) detail a simple method for estimating **in-situ** bearing support force coefficients in **flexible rotor-bearing systems**. The model neither adds mathematical complexity to existing rigid rotor models nor requires additional instrumentation than that already available in most high performance turbomachinery. The method requires two independent tests with known mass imbalance distributions and the measurement of the rotor motion (amplitude and phase) at locations close to the supports. A good rotor model (elastic and mass properties) must represent the (non observable or not measured) degrees of freedom. The procedure finds the bearing transmitted forces as a function of observable quantities (rotor motions at one side of the bearings). Imbalance response measurements conducted with a two-disk

flexible rotor supported on two-lobe fluid film bearings allow validation of the identification method estimations. Predicted (linearized) bearing force coefficients agree reasonably well with the parameters derived from the test data.

A commercial compressor company uses successfully the method advanced to qualify its equipment as per API requirements and for real-time assessment of bearing condition from measurements of rotor motions while the compressor is in operation.

Recent developments on the identification of force coefficients in non-linear systems

San Andrés and Delgado (2007-2009) have developed efficient methods to identify force coefficients in test systems that combine both linear and nonlinear mechanical elements. They apply the method to a SFD that integrates a contacting end seal to prevent air ingestion. The system motion is non-linear due to dry friction interaction at the mechanical seal mating surfaces. Single parameter characterization of the test system would yield an equivalent viscous damping coefficient that is both frequency and motion amplitude dependent. The algorithm takes the nonlinear test system as a combination of linear and nonlinear inputs with linear operators on a multiple-input/single output scheme (Rice and Fitzpatrick, 1991)

The identification method suited for nonlinear systems allows determining simultaneously the squeeze film damping and inertia force coefficients and the seal dry friction force. The identification procedure shows similar (within 10 %) force coefficients than those obtained with a more involved two-step procedure that first requires measurements without any lubricant in the test system to determine the dry-friction parameter. The identified SFD damping and inertia force coefficients agree well with model predictions that account for end flow effects at recirculation

grooves. The nonlinear identification procedure saves time and resources while producing reliable physical parameter estimations.

References

Tiwari, R., Lees, A.W., and Friswell, M.I., 2004, "Identification of Dynamic Bearing Parameters: A Review," Shock and Vibration Digest, **36**, pp. 99-124.

Nordmann, R., and Schollhorn, K., 1980, "Identification of Stiffness and Damping Coefficients of Journal Bearings by Means of the Impact Method," *Proc. Vibrations in Rotating Machinery: 2nd International Conference*, Inst. Mech. Eng., Cambridge, UK, pp. 231-238.

Goodwin, M. J., 1991, "Experimental Techniques for Bearing Impedance Measurement", *Journal of Engineering for Industry*, Vol. 113, Aug., pp. 335-342.

Murphy, B., and Scharrer, J., 1990, "The Rocketdyne Multifunction Tester, I: Test Method," Rotordynamic Instability Problems of High Performance Turbomachinery, Proceedings of a Workshop held at Texas A&M University.

Rouvas, C., and D. Childs, 1993, "A Parameter Identification Method for the Rotordynamic Coefficients of a High Speed Reynolds Number Hydrostatic Bearing," ASME *Journal of Vibration and Acoustics,* Vol. 115, pp. 264-270.

Instrumental Variable Filter Method

Fritzen, C. P., 1985, "Identification of Mass, Damping, and Stiffness Matrices of Mechanical Systems," ASME Paper 85-DET-91.

Massmann, H., and R. Nordmann, 1985, "Some New Results Concerning the Dynamic Behavior of Annular Turbulent Seals," Rotordynamic Instability Problems of High Performance Turbomachinery, Proceedings of a workshop held at Texas A&M University, Dec, pp. 179-194.

Diaz, S., and L. San Andrés, 1999, "A Method for Identification of Bearing Force Coefficients and its Application to a Squeeze Film Damper with a Bubbly Lubricant," STLE Tribology Transactions, Vol. 42, 4, pp. 739-746.

Field methods for In-Situ Parameter Identification

De Santiago, O., and L., San Andrés, 2004, "Identification of Bearing Force Coefficients from Measurements of Imbalance Response of a Flexible Rotor", ASME Paper GT 2004-54160

De Santiago, O., and L., San Andrés, 2004, "Identification of Bearing Force Coefficients in Flexible Rotor Systems", Eighth International Conference on Vibrations in Rotating Machinery, September 7th to 9th, 2004, University of Wales, Swansea, Wales, UK

De Santiago, O., and L., San Andrés, 2007, "Experimental Identification of Bearing Dynamic Force Coefficients in a Flexible Rotor – Further Developments," *Tribology Transactions,* v. 50(1), p. 114-126. Editor's Choice – Tribology & Lubrication Technology, June 2007, pp. 40-50.

De Santiago, O.C., and San Andrés, L., 2007, "Field Methods for Identification of Bearing Support Parameters-Part I: Identification from Transient Rotor Dynamic Response due to Impacts," ASME J. Eng. Gas Turbines Power, **129**, pp. 205-212.

De Santiago, O.C., and San Andrés, L., 2007, "Field Methods for Identification of Bearing Support Parameters-Part II: Identification from Rotor Dynamic Response due to Imbalances," ASME J. Eng. Gas Turbines Power, **129**, pp. 213-219.

Nonlinear-Linear System Parameter Identification

Rice, H.J., and Fitzpatrick, J.A., 1991, "Procedure for the Identification of Linear and Non-Linear Multi-Degree-of-Freedom Systems," J. Sound Vib., **149**(3), pp. 397-411

San Andrés, L., and Delgado, A., 2007, "Identification of Force Coefficients in a Squeeze Film Damper with a Mechanical End Seal- Centered Circular Orbit Tests," ASME J. Tribol., **129**(3), pp. 660-668.

Delgado, A., and San Andrés, L., 2008, "Nonlinear Identification of Mechanical Parameters in a Squeeze Film Damper with Integral Mechanical Seal," ASME paper No. GT2008-50528. (Scheduled for publication in J. Eng. Gas Turbines Power, September 2009, vol. 131)

Delgado, D., and San Andrés, L., 2009, "Identification of Squeeze Film Damper Force Coefficients from Multiple-Frequency, Non-Circular Journal Motions," ASME paper No**.** GT2009-59175(Scheduled for publication in J. Eng. Gas Turbines Power, 2010, vol. 132)

An example of system parameter identification (Hybrid Brush Seal)

Luis San Andrés (lecturer)

Thanks to Adolfo Delgado, José Baker (RAs) &
support from Siemens Power Generation

Experimental Facility

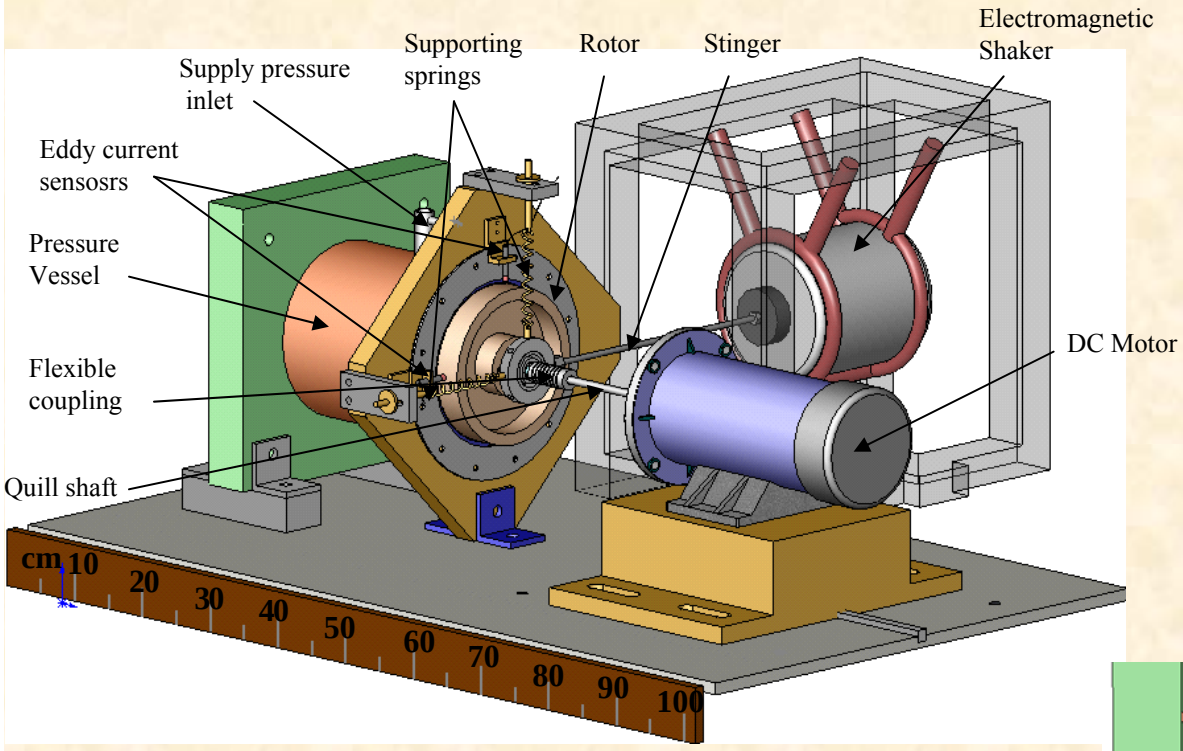

Structural parameters

K_{shaft}= 243 lbf/in (42.5 kN/m)

M_{s+d}= 9.8 lb (4.45 kg)

ζ: 0.01 % (damping ratio)

Installation:

6.550” diameter brush seal

Max. air Pressure: 60 psig

Shaker (20 lb max)

Test Rig: Rotordynamic Configuration

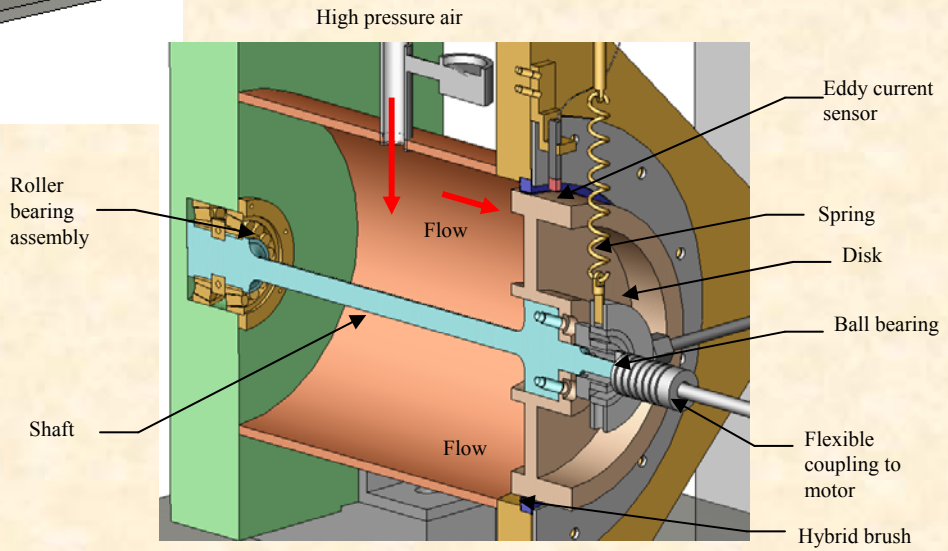

Detail view of brush seal test rig

GT2008-50532

Brush Seals

Reduce secondary leakage in turbomachinery
Replace labyrinth seals in HP TM (hot side of steam & gas turbines)
Wear and thermal distortions are a reliability problem

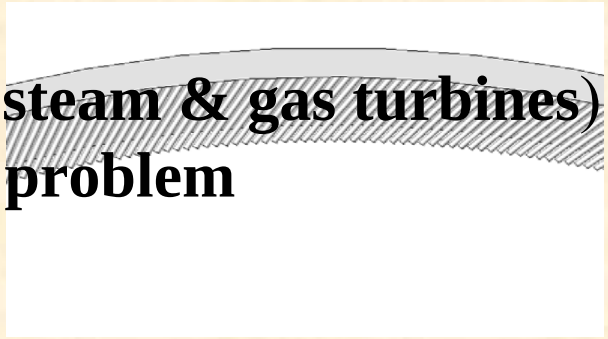

Hybrid Brush Seals

Novel improvement over BS. Reduce more leakage and do not introduce wear or thermal distortion. Allow bi-directional rotation

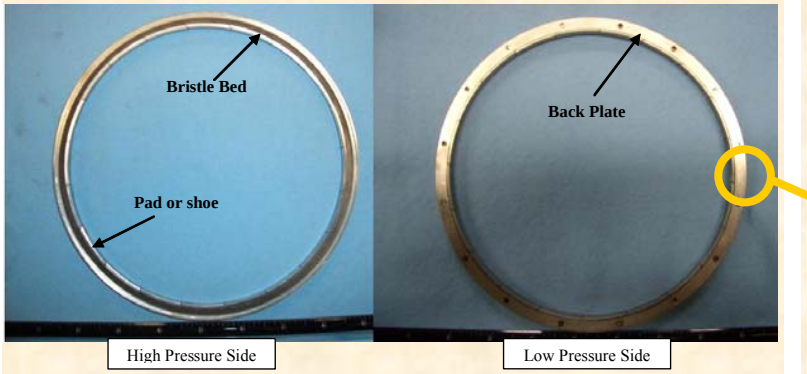

Courtesy of Advanced Turbomachinery Group®

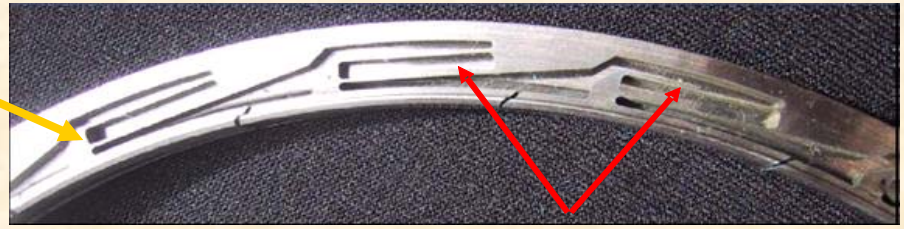

*** Close-up courtesy of Advanced Technologies Group, Inc.**

Spring Lever Mechanism

Dynamic Load Tests (no shaft rotation)

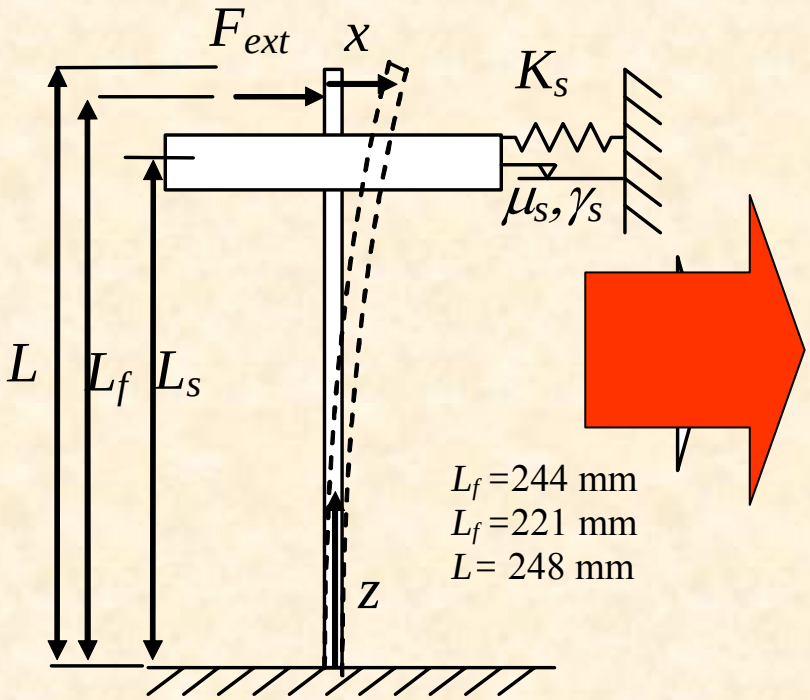

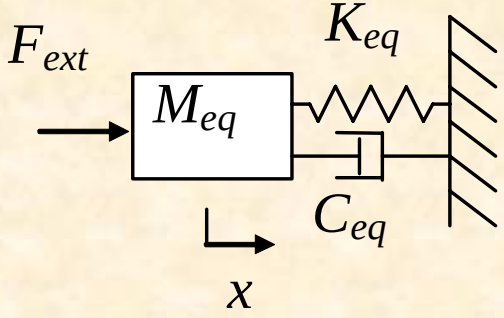

Equivalent Test System

$$M_{eq}\ddot{x} + K_{eq}x + C_{eq}\dot{x} = F_{ext}$$

Parameter Identification (no shaft rotation)

ASME DETC2005-84159

$$\bar{x} = xe^{i\omega t} \qquad \bar{F} = F_{ext}e^{i\omega t}$$

Harmonic force & displacements

$$Z = \frac{\bar{F}}{\bar{x}} = (K_{eq} - \omega^2 M_{eq}) + i\,\omega C_{eq}$$

Impedance Function

$$W = \oint F_{ext}\,\dot{x}\,dt$$

Work External

$$E_{dis} = \pi\omega C_{eq}\left|\bar{x}\right|^2$$

Viscous Dissipation

$$E_{dis} = \gamma_{eq}\pi K_{eq}\left|\bar{x}\right|^2 + 4\mu\left|\bar{F}\right|\left|\bar{x}\right|$$

DRY FRICTION & STRUCTURAL DAMPING

HBS Dynamic Stiffness vs. Frequency (no shaft rotation)

Load = 63 N, frequency: 20-100Hz

Pressure ratio ($P_r = P_s/P_d$) = Discharge/Supply

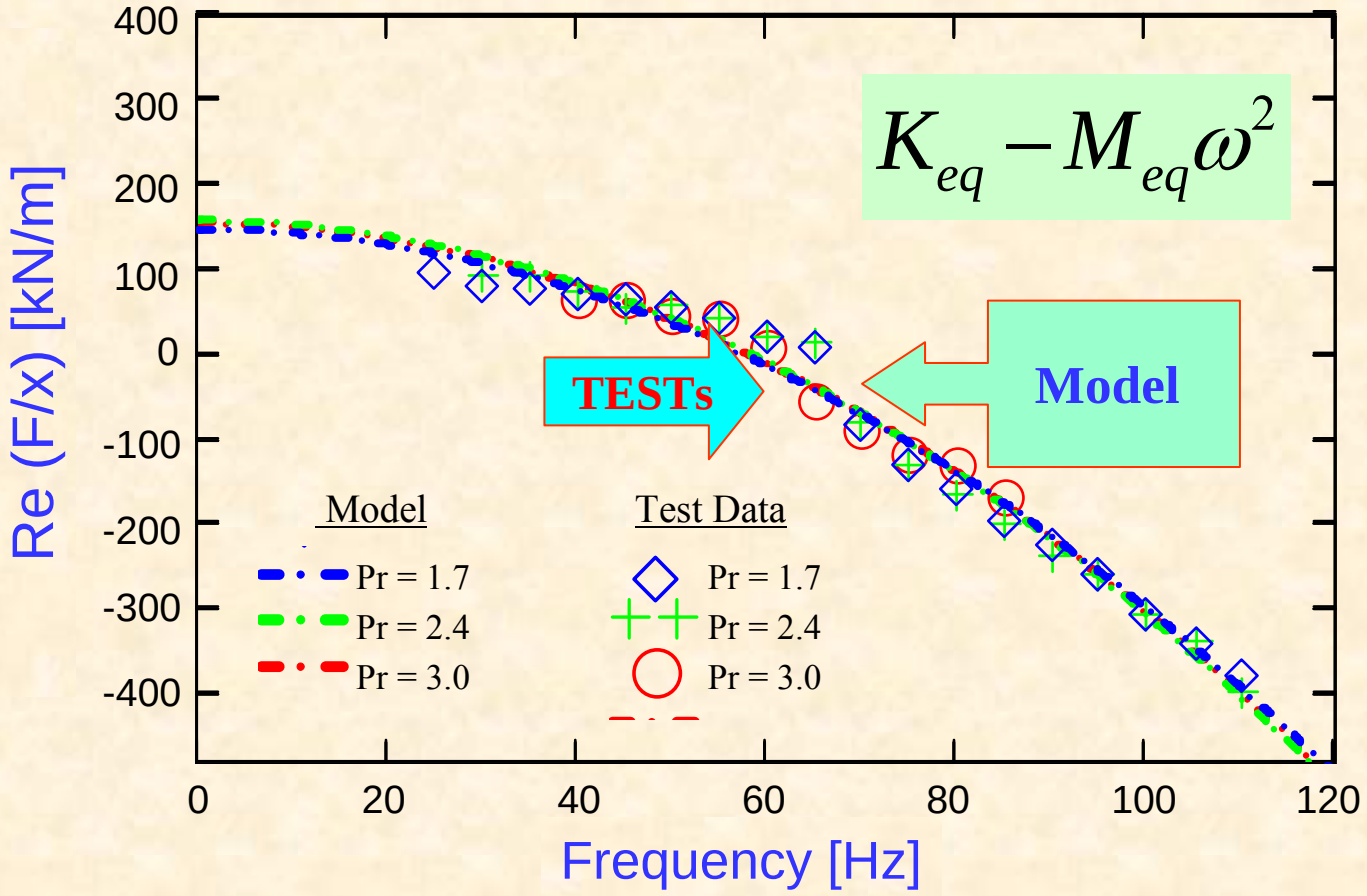

Model reproduces real part of the impedance under the given supply pressure conditions.

HBS Equivalent Viscous Damping vs. Frequency (no shaft rotation)

Load = 63 N, frequency 20-110Hz

Pressure ratio ($P_r = P_s/P_d$) = Discharge/Supply

$$C_{eq} = \frac{\gamma_{eq} K_{eq}}{\omega} + \frac{4\mu|\bar{F}|}{\pi\omega|\bar{x}|}$$

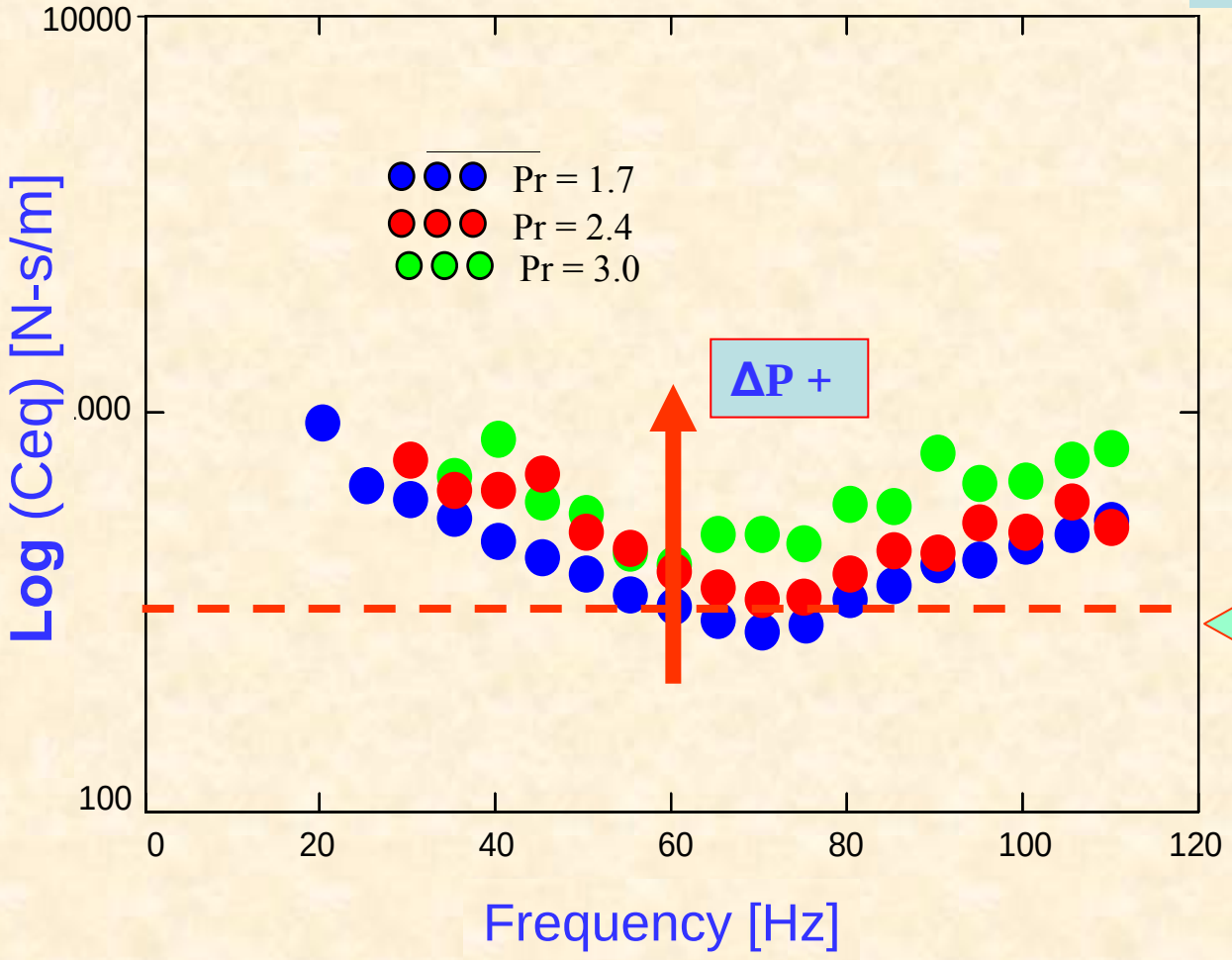

Equivalent damping increases slightly with pressure differential. Results typical of a system with dry-friction & material damping energy dissipation

Viscous Model

Identification of Rotordynamic Force Coefficients

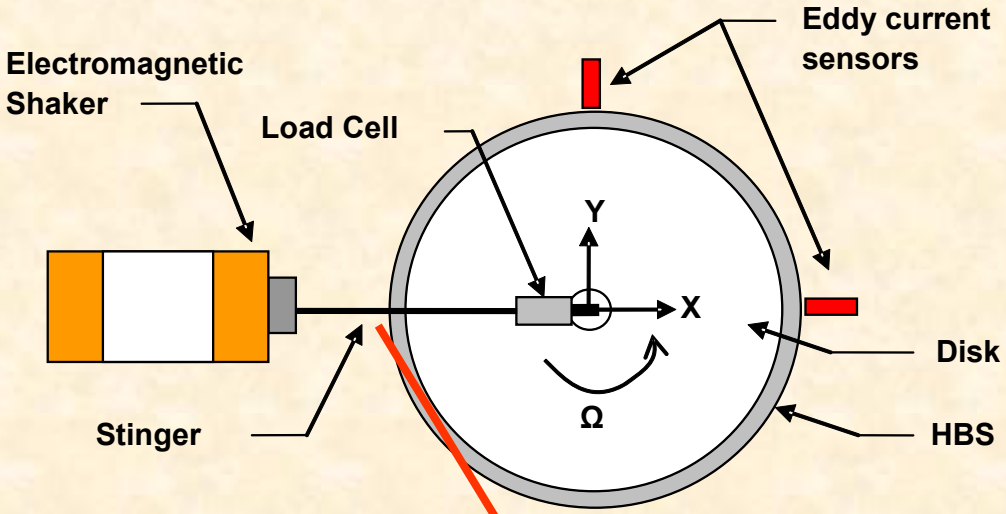

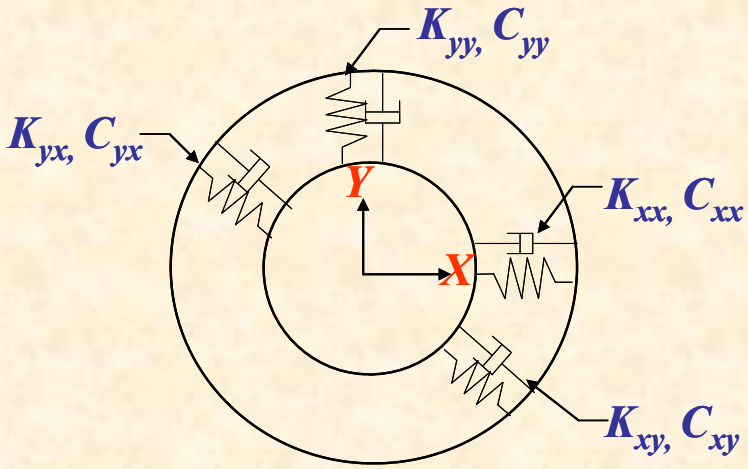

Excitation force (frequency ω)

$$\begin{bmatrix} M_{xx} & M_{xy} \\ M_{yx} & M_{yy} \end{bmatrix} \begin{Bmatrix} \ddot{x} \\ \ddot{y} \end{Bmatrix} + \begin{bmatrix} K_{xx} & K_{xy} \\ K_{yx} & K_{yy} \end{bmatrix} \begin{Bmatrix} x \\ y \end{Bmatrix} + \begin{bmatrix} C_{xx} & C_{xy} \\ C_{yx} & C_{yy} \end{bmatrix} \begin{Bmatrix} \dot{x} \\ \dot{y} \end{Bmatrix} = \begin{pmatrix} F_x \\ 0 \end{pmatrix} + \begin{pmatrix} F_{ix} \\ F_{iy} \end{pmatrix}$$

Imbalance forces (1X=Ω)

Identification of Rotordynamic Force Coefficients

For periodic force excitation:

$$\bar{F}_x = F_x e^{i\omega t} \Rightarrow \begin{matrix} \bar{y} = y e^{i\omega t} \\ \bar{x} = x e^{i\omega t} \end{matrix}$$

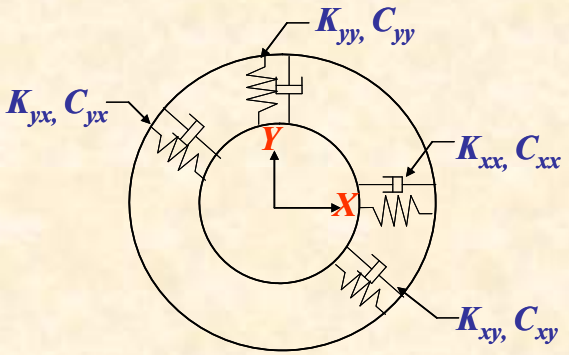

EOMS reduce to:

$$Z_{xx} \cdot \bar{x} + Z_{xy} \cdot \bar{y} = \bar{F}_x$$

$$Z_{yx} \cdot \bar{x} + Z_{yy} \cdot \bar{y} = 0$$

With **impedances**:

$$Z_{\alpha\beta} = \left\{ K_{\alpha\beta} - M_{\alpha\beta}\omega^2 + iC_{\alpha\beta}\omega \right\}, \alpha\beta = x, y$$

For centered operation (axi-symmetry)

$$Z_{xx} = Z_{yy} \qquad Z_{xy} = -Z_{yx}$$

$$\begin{bmatrix} M_{xx} & 0 \\ 0 & M_{xx} \end{bmatrix} \begin{Bmatrix} \ddot{x} \\ \ddot{y} \end{Bmatrix} + \begin{bmatrix} K_{xx} & K_{xy} \\ -K_{xy} & K_{xx} \end{bmatrix} \begin{Bmatrix} x \\ y \end{Bmatrix} + \begin{bmatrix} C_{xx} & 0 \\ 0 & C_{xx} \end{bmatrix} \begin{Bmatrix} \dot{x} \\ \dot{y} \end{Bmatrix} = \begin{pmatrix} F_x \\ 0 \end{pmatrix}$$

Rotor mode shapes

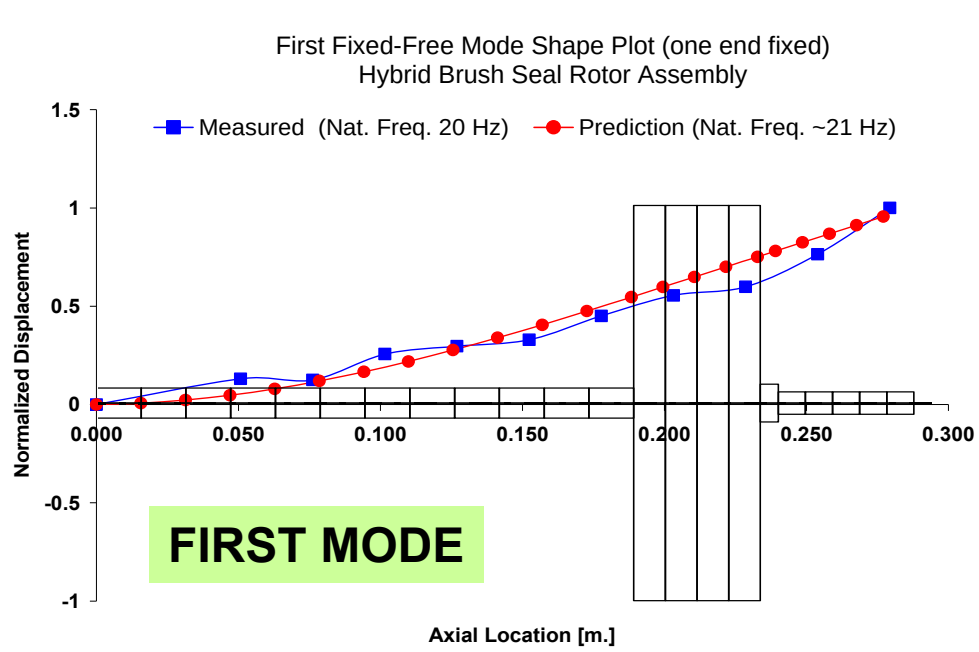

Only first mode excited in rotor speed range (0-1200 rpm)

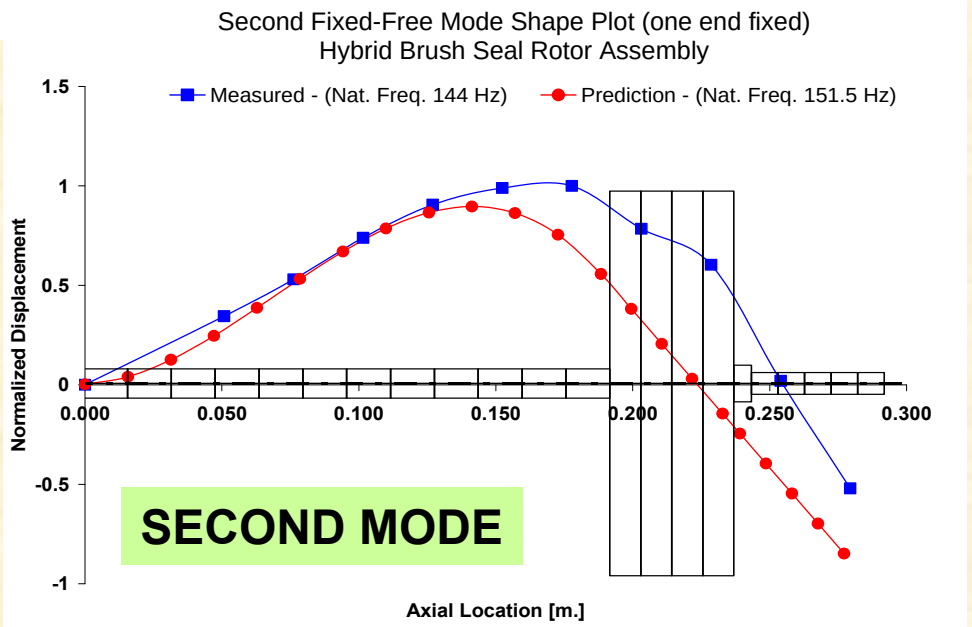

Effect of rotor speed on rotor-HBS natural frequency

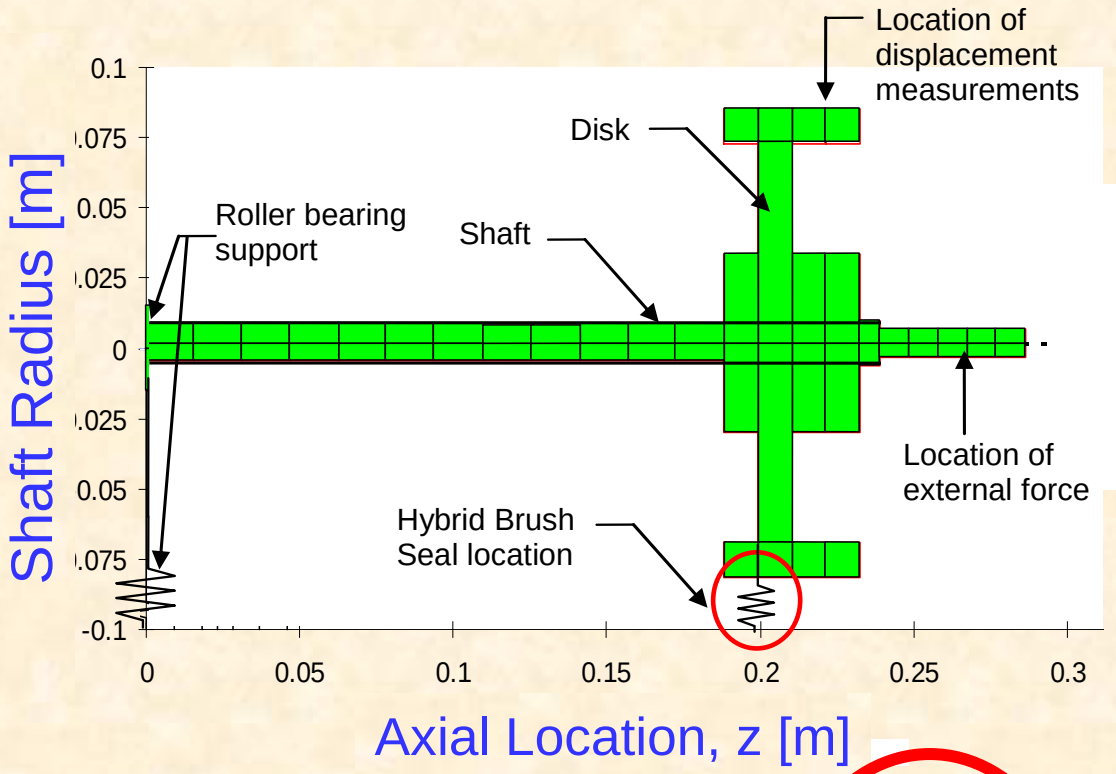

Gyroscopic effects negligible for test rotor speeds (600 and 1,200 rpm [20 Hz])

Rotor Speed [RPM]	1st Backward Nat. Frequency, [Hz]	1st Forward Nat. Frequency, [Hz]	2nd Forward Nat. Frequency, [Hz]	3rd Forward Nat. Frequency, [Hz]
0	30.5	30.5	146	1351
600	29.7	31.4	154	1351
1200	28.8	32.2	163	1351

T=32 Hz

CROSS-Coupling Effects under rotation

Load=22 N, 600 rpm

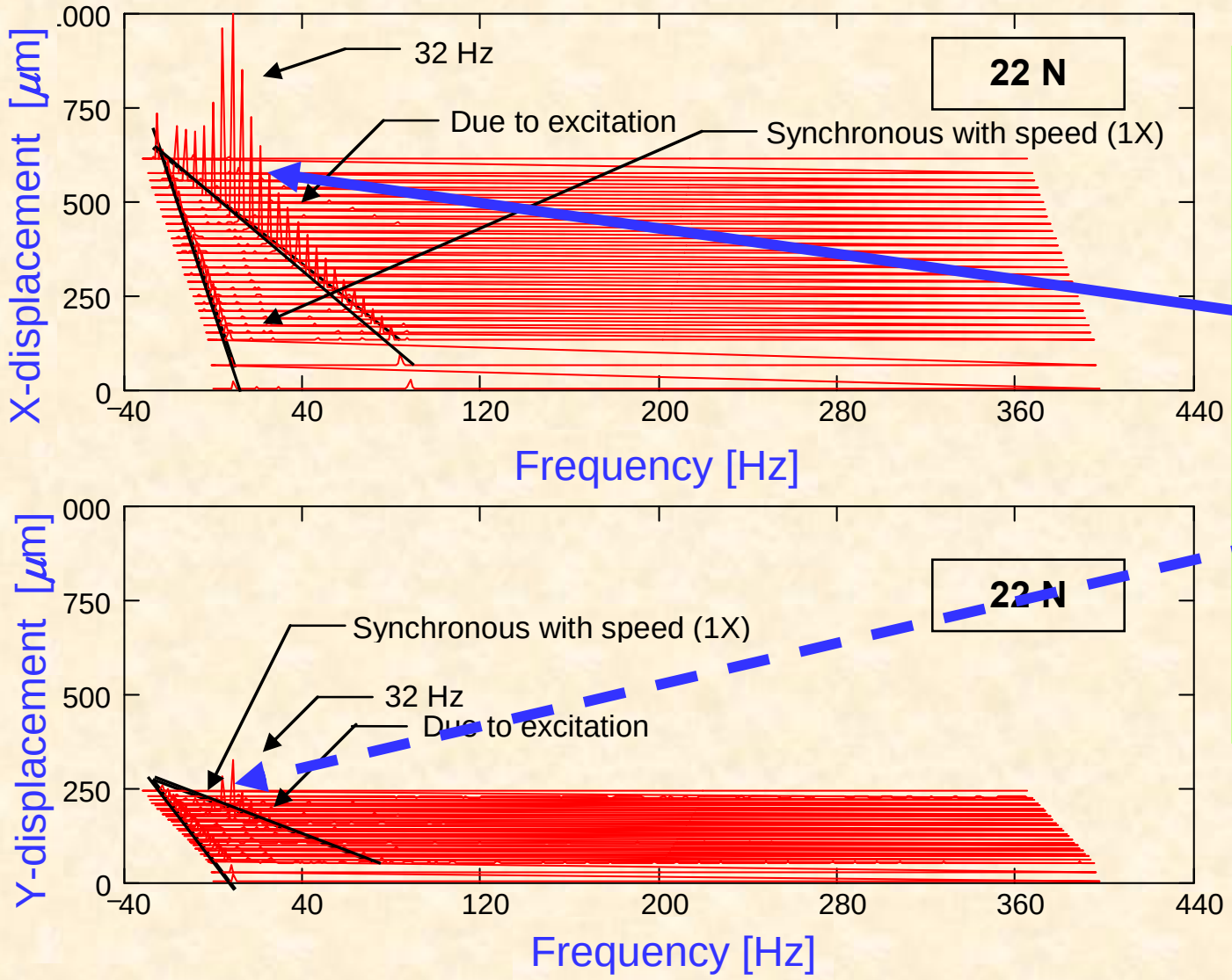

For load along *X* direction, rotor principal (*X*) motions >>> cross (*Y*) motions

***3X* motions always small**

Test dynamic stiffness vs. frequency

Load = 22 N, frequency 25-80Hz

Pressure ratio ($P_r = P_s/P_d$) = Discharge/Supply

$$Z_{xx} = \frac{\bar{F}_x \cdot \bar{x}}{(\bar{x}^2 + \bar{y}^2)}$$

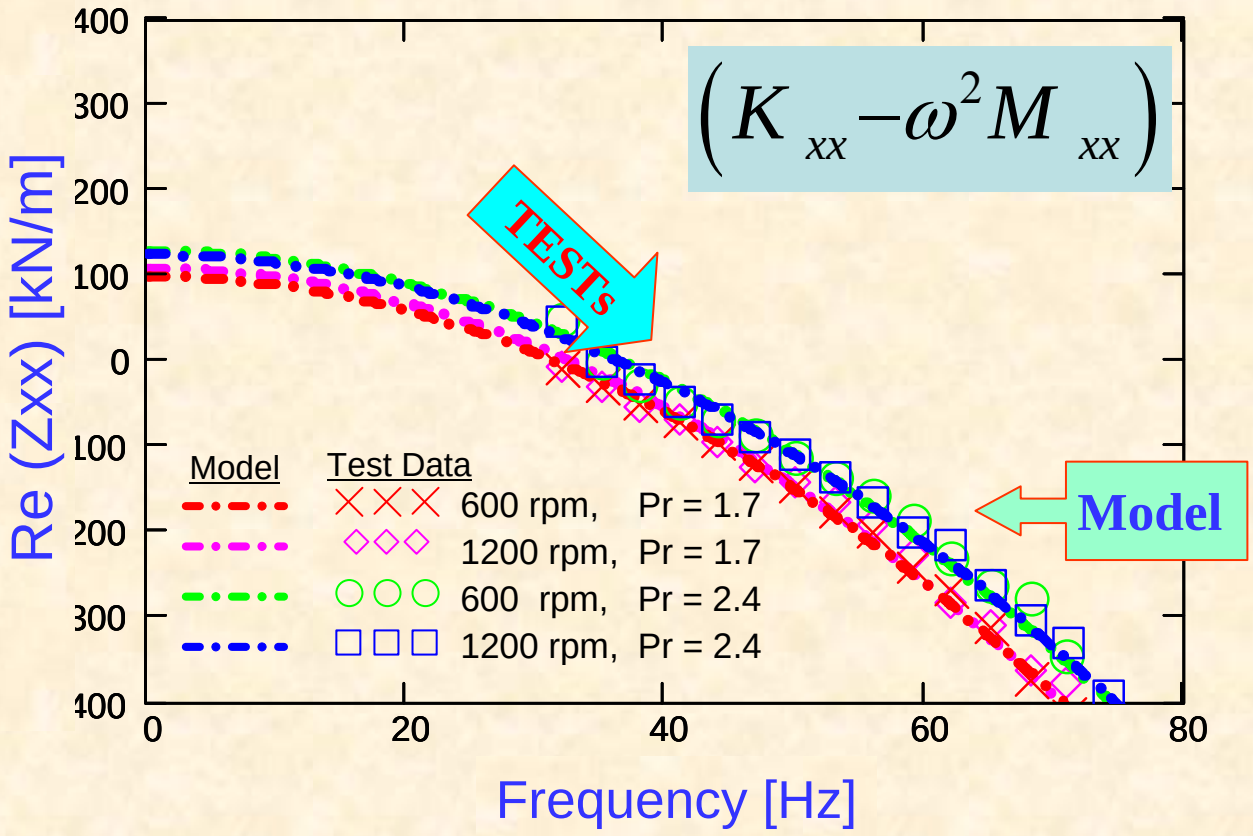

Model reproduces the measured real part of impedance. Little effect of pressurization

Test impedance (imag) vs. frequency

Load = 22 N, frequency 25-80Hz

Pressure ratio ($P_r = P_s/P_d$) = Discharge/Supply

$$Z_{yx} = -Z_{yy}\,\frac{\bar{y}}{\bar{x}}$$

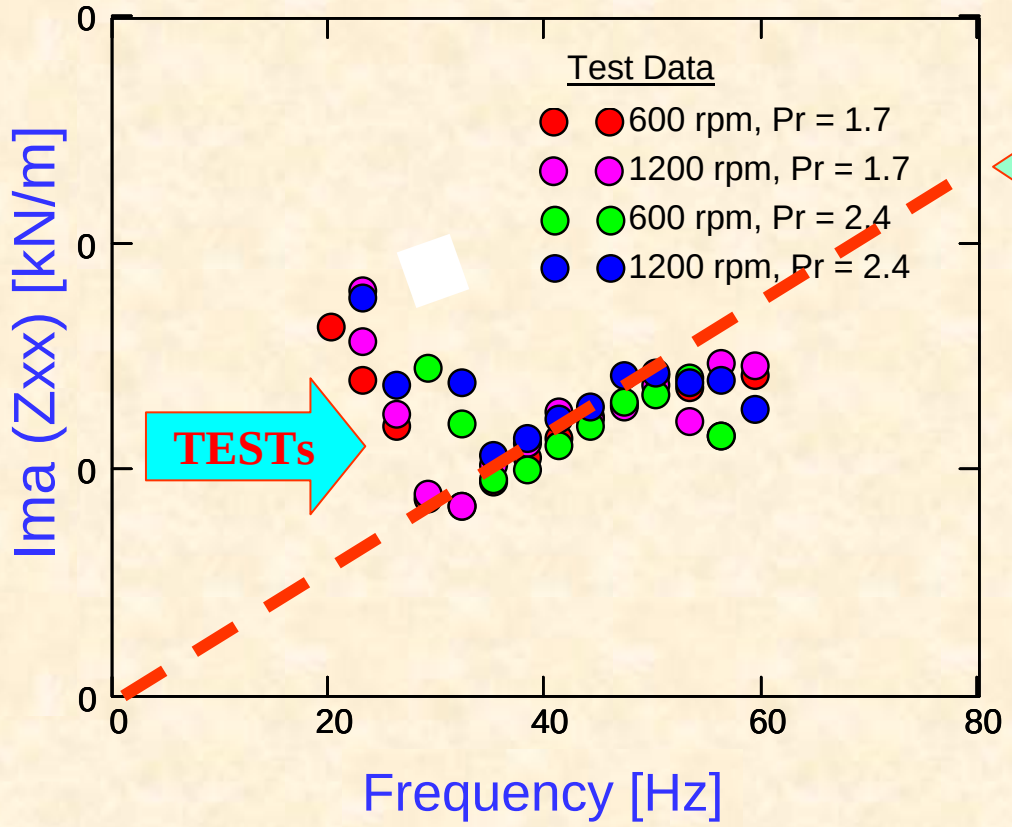

Damping is NOT viscous

Equivalent Viscous Damping (C_{xx}~C_{eq}) vs. Frequency

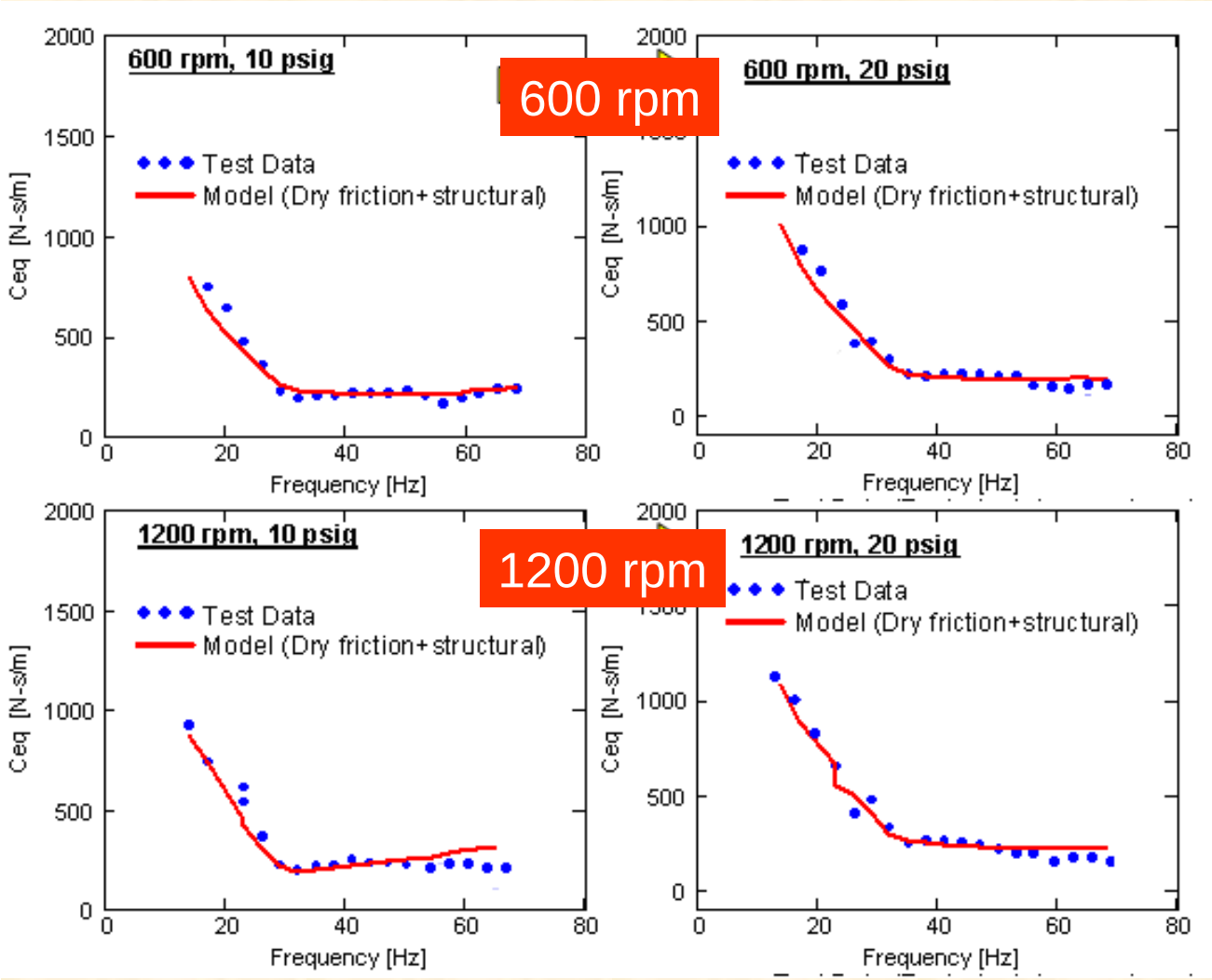

Damping decreases with frequency, with little effect of supply pressure. Minimum value at test system natural frequency (~32 Hz)

Pr=1.7

Pr=2.4

HBS predicted & test direct stiffness vs. frequency

Frequency 25-100 Hz

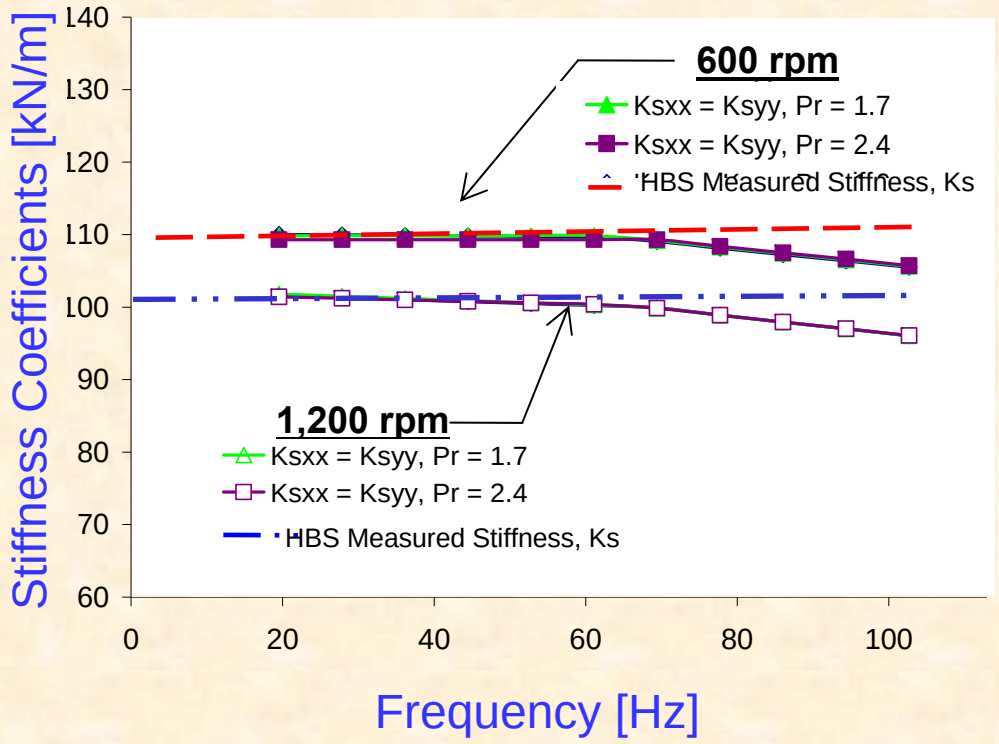

Predicted HBS stiffness (K_{sxx}) drops slightly in range from 20- 100 Hz. Tests show nearly constant K_{sxx}

Pressure ($P_r = P_s/P_d$) has negligible effect on seal direct stiffness, K_{sxx}

ASME GT2004-53614

Code: XLTPGASBEAR

HBS predicted & test cross stiffness vs. frequency

Frequency 25-100 Hz

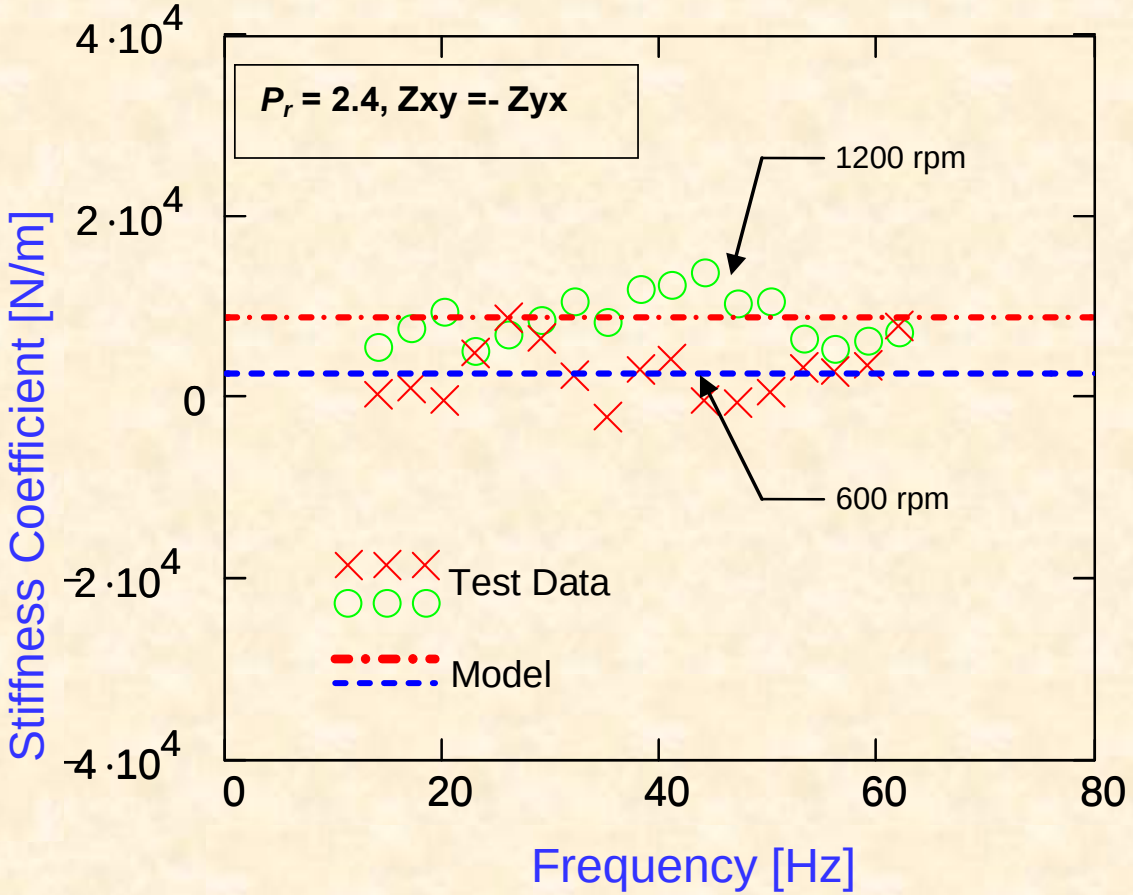

$$Z_{yx} = -Z_{xx}\frac{\overline{y}}{\overline{x}}$$

HBS cross stiffness (K_{sxy}) << direct stiffness (K_{sxx})

Pressure ($P_r = P_s/P_d$) has negligible effect on seal cross stiffness, K_{sxy}

HBS predicted & test damping vs. frequency

Frequency 25-100 Hz

Pressure ratio ($P_r = P_s/P_d$) = Discharge/Supply

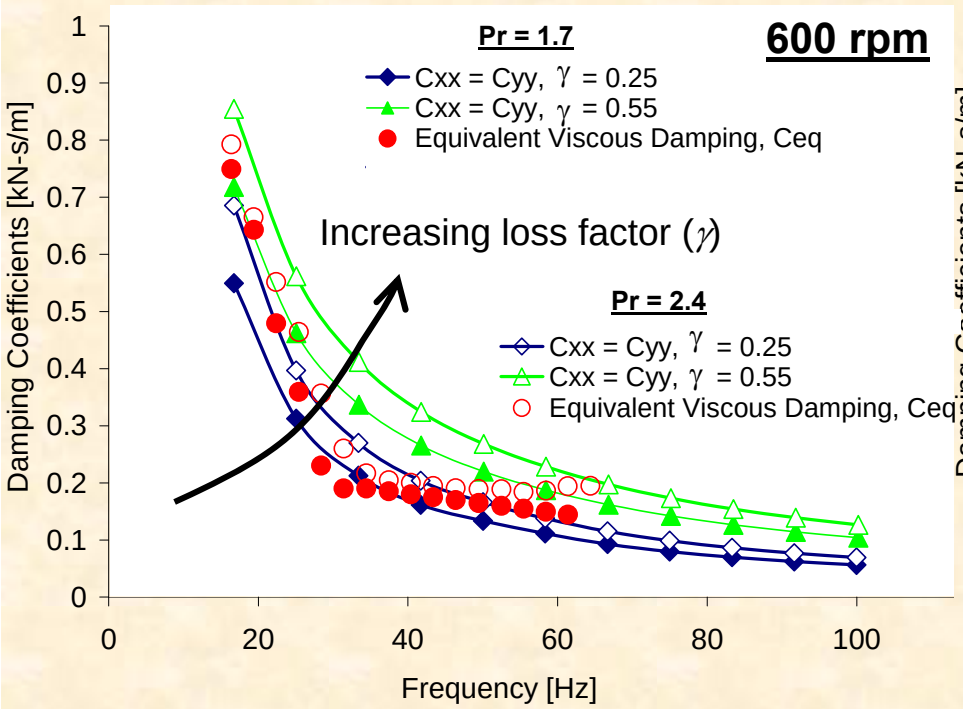

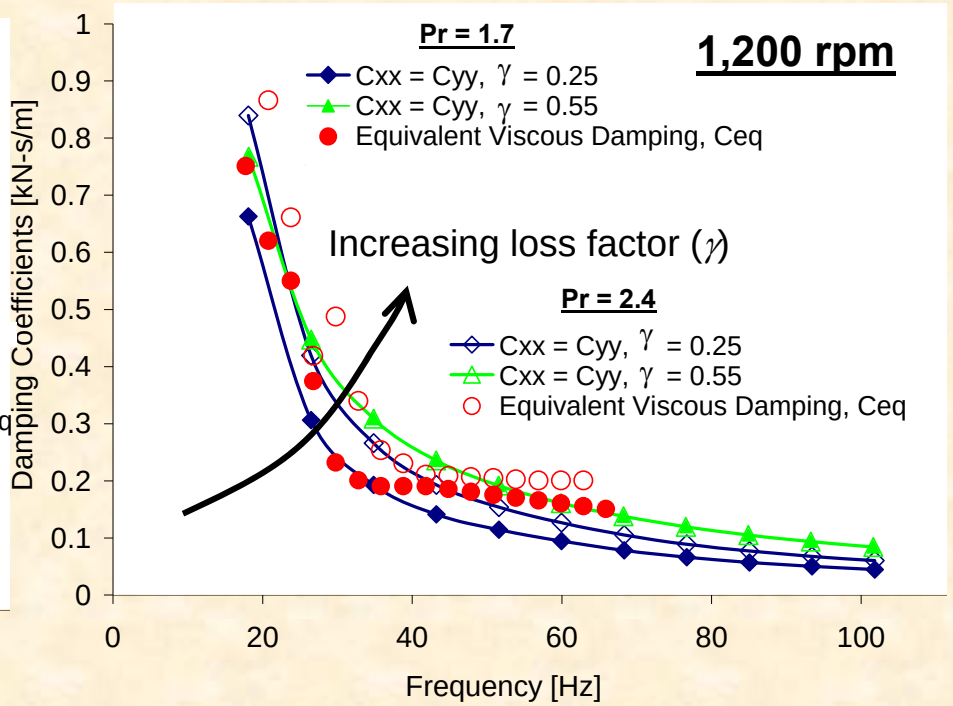

HBS direct damping (C_{sxx}) decreases with excitation frequency. Loss factor coefficient (γ) models well seal structural (hysteresis) damping

Conclusions

- A structural loss factor (γ) and a dry friction coefficient(μ) effectively characterize the energy dissipation mechanism of a Hybrid Brush Seal (HBS).

- HBS Direct stiffness ($K_{sxx} = K_{syy}$) decreases minimally with rotor increasing rotor speed for $P_r = 1.7$ and 2.4 HBS Cross-coupled stiffness ($K_{sxy} = -K_{syx}$) is much smaller than the direct stiffness coefficients.

- HBS Direct viscous damping coefficients decrease as a function of increasing excitation frequency.